Cellulose (2023) 30:8355–8368
https://doi.org/10.1007/s10570-023-05373-8

ORIGINAL RESEARCH

Thermoresponsive hydrogels with sulfated polysaccharide-derived copolymers: the effect of carbohydrate backbones on the responsive and mechanical properties

Kui Zeng · Dan Xu · Shuaiyu Gong · Yi-Tung Lu · Philipp Vana · Thomas Groth · Kai Zhang

Received: 18 February 2023 / Accepted: 2 July 2023 / Published online: 20 July 2023

Abstract Thermoresponsive hydrogels based on ionic cellulose/chitosan are widely used various fields, such as smart windows and tissue engineering, while the effect of carbohydrate backbones of cellulose/chitosan on the thermal response and mechanical properties of hydrogels has received less attention so far. Herein, poly(2(dimethylamino) ethyl methacrylate) (PDMAEMA)-grafted cellulose sulfate (P-CS) and PDMAEMA-grafted chitosan sulfate (P-CHS) as research models are successfully synthesized through multi-step reactions. The P-CS and P-CHS polymers are further applied in crosslinked polyacrylamide networks, resulting in the P-CS and P-CHS hydrogels. Compared to P-CS hydrogels, P-CHS hydrogels could obviously block the transmission of visible light when the temperature is changed from 25 to 42 °C. In contrast to P-CHS hydrogels, the P-CS hydrogels change easily from soft and weak state to stiff and strong state according to their mechanical behaviors. These results indicate that different carbohydrate backbones of cellulose and chitosan should have caused distinct aggregation behaviors of corresponding P-CS and P-CHS hydrogels, which are accompanied by different light transmittance and mechanical properties.

Kui Zeng and Dan Xu have contributed equally to this work.

Supplementary Information The online version contains supplementary material available at https://doi.org/10.1007/s10570-023-05373-8.

K. Zeng · D. Xu · S. Gong · K. Zhang (✉)
Department of Wood Technology and Wood-Based Composites, Sustainable Materials and Chemistry, University of Göttingen, Büsgenweg 4, 37077 Göttingen, Germany
e-mail: kai.zhang@uni-goettingen.de

Y.-T. Lu · T. Groth
Department Biomedical Materials, Institute of Pharmacy, Martin Luther University Halle-Wittenberg, Heinrich-Damerow-Strasse 4, 06120 Halle (Saale), Germany

P. Vana
Institute of Physical Chemistry, University of Göttingen, Tammannstraße 6, 37077 Göttingen, Germany

T. Groth
Interdisciplinary Center of Material Science, Martin Luther University Halle-Wittenberg, 06099 Halle (Saale), Germany

Graphical abstract Thermoresponsive hydrogels using PDMAEMA-grafted ionic cellulose sulfate (P-CS) and chitosan sulfate (P-CHS) are successfully prepared. Distinct carbohydrate backbone displayed different effects on the thermoresponsive and mechanical properties of hydrogels.

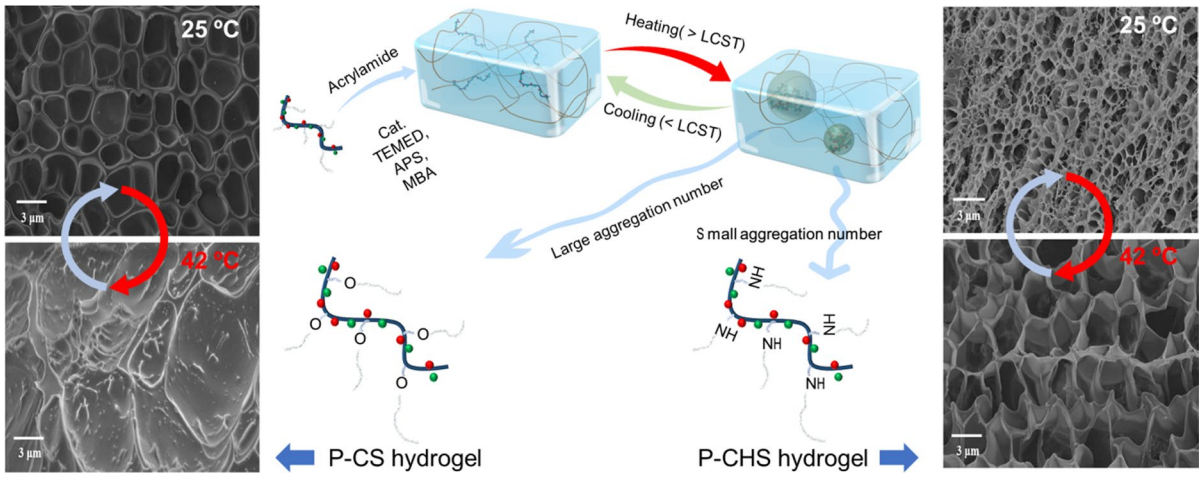

Keywords Thermoresponsive · Hydrogel · PDMAEMA · Cellulose sulfate · Chitosan sulfate

Introduction

Thermoresponsive hydrogels, as one type of important stimuli-responsive materials, have shown a wide range of applications in smart category (Ke et al. 2019), tissue engineering (Doberenz et al. 2020), drug delivery (Hoffman 2013), sensors (Xiong et al. 2013) and devices (Li et al. 2018; Wang et al. 2020). To date, there are a number of thermoresponsive polymers for diverse purposes, such as poly-*N*-isopropylacrylamide (Okano et al. 1993), Pluronics (Schmolka 1972), elastin-like polypeptides (Vrhovski and Weiss 1998), poly(*N*-vinylcaprolactam) (Meeussen et al. 2000) and poly(2(dimethylamino)ethyl methacrylate) (PDMAEMA) (Van de Wetering et al. 1998). The last is a polycation containing tertiary amine groups and possessing bioactive properties (Rawlinson et al. 2010). It is a weak polybase that has interesting temperature dependent solubility, so that PDMAEMA and its copolymers are currently widely used in thermoresponsive hydrogels in various fields, e.g. therapeutic drug delivery, biotechnology, medicine and pharmacy (Ma et al. 2001; Wang et al. 2014). Despite the substantial progress in the construction of diverse thermoresponsive hydrogels, there is still highly desired for hydrogels with low toxic, biocompatible, degradable, inexpensive and abundant advantages.

As important materials from living organisms, cellulose (Stamm 1964) composed of D-glucose residues and chitosan (Ahmed and Ikram 2017) composed of *N*-acetyl-D-glucosamine residues and D-glucosamine residues linked with β-(1–4) glucoside bonds are the most abundant sustainable natural polymers with all the aforementioned advantages (Ahmed and Ikram 2017; Stamm 1964). Hence, it is attractive to fabricate cellulose/chitosan-based thermoresponsive hydrogels for diverse applications (Coviello et al. 2007; Yang et al. 2021; Zainal et al. 2021). Until today, ionic or nonionic cellulose/chitosan-based thermoresponsive materials (Kabir et al. 2018; Yang et al. 2021) have been utilized for smart windows (Bi et al. 2020; Ding et al. 2020), tissue engineering (Klouda and Mikos

2008; Lu et al. 2022, 2023; Zeng et al. 2022; Zou et al. 2022), controlled delivery of proteins and peptides (Dragan and Dinu 2019), multifunctional electrical skins (Zhang et al. 2020), whereas the effect of carbohydrate backbones of cellulose and chitosan on thermoresponsive and mechanical properties of these thermoresponsive hydrogels has received less attention so far.

Sulfated cellulose/chitosan with ionic characters as mimic of native heparin and heparin sulfate (Zeng et al. 2019) are readily water-soluble and can be readily crosslinked, making the hydrogel network sensitive to various internal and external variables, such as pH, ions and temperature, etc. (Alvarez-Lorenzo et al. 2013). Therefore, to prepare thermoresponsive hydrogels, PDMAEMA-grafted cellulose sulfate (P-CS) and PDMAEMA-grafted chitosan sulfate (P-CHS) were first time synthesized and were chosen as the model for the study. Thermoresponsive, optical and mechanical properties of P-CS and P-CHS hydrogels were then investigated and compared, which will elucidate the effects of carbohydrate backbones on the fabricated hydrogel materials and guide future preparation of responsive hydrogels with desired functionalities.

Materials and methods

Materials

Unless otherwise specified, the chemicals were obtained commercially and used without further purification. It will be mentioned if there is any further purification for the chemicals. Commercial microcrystalline cellulose Avicel PH-101 (MCC) was purchased from Sigma Aldrich. Chitosan was purchased from HEPPE MEDICAL CHITOSAN GmbH. The degree of deacetylation (DD) of chitosan is 97.96% (DD: 97.96%). All reactions were performed under an atmosphere of Ar using standard Schlenk line unless specified otherwise. All glassware was dried at 120 °C beforehand. Before use, 2-(dimethylamino)ethyl methacrylate (DMAEMA) was freshly filtered through the basic aluminum oxide to remove inhibitors. The initiator, azobisisobutyronitrile (AIBN), was recrystallized from methanol. Solvents (toluene, THF, DMF) were dried with a 4 Å molecular sieve.

Preparation of PDMAEMA

A mixture of monomer DMAEMA (4.716 g, 30 mmol, 100 equiv.), chain transfer agent cyanopantanoic acid dithiobenzoate (CPADB) (83.81 mg, 0.3 mmol, 1.0 equiv.), initiator AIBN (9.85 mg, 0.06 mmol, 0.2 equiv.) in toluene (15 mL) was charged to Schlenk tube. The mixture was degassed by three freeze-evacuate-thaw cycles. Then, the tube was sealed and heated in an oil bath at 75 °C under argon gas atmosphere. After 6 h of polymerization, the reaction was quenched by cooling down in ice water and exposing to air. The PDMAEMA-CTA was isolated by precipitating in cold *n*-hexane (150 mL). In order to remove the monomer sufficiently, the polymer was re-dissolved in chloroform and precipitated from cold *n*-hexane for two more times. The obtained yellow oil precipitate, which is oligomer PDMAEMA with a chain transfer agent residual, named PDMAEMA-CTA, was collected and dried under vacuum overnight with the yield of 29 wt%. ^{1}H NMR (500 MHz, D_2O): δ 7.85 (d, H of Ar), 7.52–7.49 (m, H of Ar), 7.36–7.34 (m, H of Ar), 4.05 (d, H of PDMAEMA), 2.57 (d, H of PDMAEMA), 2.27 (s, H of PDMAEMA), 1.97–1.75 (m), 1.37–1.20 (m), 1.04 (s), 0.87 (s). FT-IR (ATR) in cm^{-1}: $\tilde{\nu} = 1722$ (C=O), 1145 (C–N). Molecular weight (analysis with GPC): $M_n = 5733$ Da; $M_w = 6560$ Da; PDI = 1.14.

Preparation of cellulose sulfate

First, cellulose (2.5 g, 15.4 mmol AGU, 1.0 equiv.) was suspended in anhydrous DMF (125 mL) in a 500 mL flask. The mixture was stirred under room temperature for over 14 h (Hettrich et al. 2008; Zhang et al. 2009). Then the sulfating reagent was prepared by dropping chlorosulfuric acid (6.171 mL, 92.8 mmol, 6.0 equiv.) into DMF (25 mL) under an ice water bath and argon atmosphere within 5 min, followed by slowly adding acetic anhydride (5.835 mL, 61.7 mmol, 4.0 equiv.). Subsequently, the sulfating reagent was added to the cellulose suspension dropwise under cooling. After filled with argon and sealed, the flask was placed in oil bath at 40 °C for 5 h. Thereafter, the mixture was poured into saturated ethanolic solution (600 mL) of anhydrous sodium acetate. The precipitate was obtained by centrifuging and washing with 125 mL 4% sodium

acetate solution in ethanol, followed by deacetylating with 1 M ethanolic solution of sodium hydroxide over 15 h. After centrifugation again, the precipitate was dissolved in deionized water (DI-water) overnight. The pH-value was adjusted to 8.0 with acetic acid/ethanol (50/50, m/m) and the solution was filtered. The product was dialyzed (in dialysis membrane with a MWCO = 3.5 kDa) against ultrapure water for 1 week and then lyophilized into dry product. ^{13}C NMR (125 MHz, D_2O): δ 102.28 (C_1), 100.20 (C_{1S}), 78.07 (C_4), 74.27–71.76 (C_3, C_2, C_5), 66.10 (C_{6S}), 59.78 (C_6). FT-IR (ATR) in cm^{-1}: $\tilde{\nu}$ = 1205 (S=O), 814 (S–O). Degree of substitution ascribed to sulfate group is DS_S = 1.0. Details of calculation methods of the DSs and elemental analysis results can be found in Supporting Information.

Preparation of chitosan sulfate

Chitosan (1.0 g, 6.2 mmol units, 1.0 equiv.) was dissolved in formic acid (20 mL) within 1 h under stirring, followed by adding anhydrous DMF (156 mL) and stirring for 2 h (Zhang et al. 2010a, b). The sulfating reagent was prepared by slowly dropping chlorosulfuric acid (2.476 mL, 37.2 mmol, 6 equiv.) into DMF (10 mL) within 10 min under cooling and argon atmosphere. Then the sulfating reagent was added to the chitosan solution dropwise within 30 min and the mixture was kept at 50 °C for 5 h. After the designated reaction time, the yellow solution was poured into saturated ethanolic solution (600 mL) of anhydrous sodium acetate. The precipitate was washed with ethanol/water-solution (4/1, v/v) and dissolved in DI-water under stirring overnight. The pH value was adjusted to 7.5 with 0.5 M sodium hydroxide solution. The product was dialyzed (in dialysis membrane with a MWCO = 3.5 kDa) against ultrapure water for 1 week and then lyophilized into dry product. ^{13}C NMR (125 MHz, D_2O) δ 97.50 (C_1), 96.32 (C_{1S}), 78.11 ($C_{3,3S}$), 75.88–73.85 ($C_{4,4S}$), 72.72 ($C_{5,5S}$), 66.58 (C_{6s}), 60.00 (C_6), 54.98 (C_2). FT-IR (ATR) in cm^{-1}: $\tilde{\nu}$ = 1203 (S=O), 795 (S–O). Degree of substitution ascribed to sulfate group is DS_S = 1.67. Details of calculation methods of the DSs and elemental analysis results can be found in Supporting Information.

Preparation of poly(2(dimethylamino)ethyl methacrylate) (PDMAEMA)-grafted cellulose sulfate (P-CS)

In order to prevent the oxidation of the thiol group after aminolysis, one-pot synthesis was applied by conducting the aminolysis immediately followed with introduction of PDMAEMA on cellulose sulfate. The obtained PDMAEMA-SH solution (0.6 g, 0.105 mmol) was degassed sufficiently with argon gas, followed by mixing it with cellulose sulfate acrylate (175.55 mg, 0.7 mmol, the details for the preparation of cellulose sulfate acrylate was included in Supporting Information) solution. After adding 4-dimethylaminopyridine (17.10 mg, 0.14 mmol) promptly and repeated degassing, the reaction was preceded by irradiating with 365 nm UV light for 24 h. The obtained mixture solution was concentrated with rotary evaporator and dialyzed (in dialysis membrane with a MWCO = 10 kDa) against ultrapure water for 1 week and then lyophilized into dry product. ^{1}H NMR (400 MHz, D_2O) δ 4.62–4.55 (m), 4.21 (s), 3.98–3.67 (m), 2.82 (s), 2.43–2.40 (m), 1.98–1.32 (m), 1.15 (s), 0.95 (s). ^{13}C NMR (126 MHz, D_2O) δ 178.53 (PDMAEMA), 177.62 (PDMAEMA), 102.33 (C_1), 101.76 (C_{1s}), 78.07 (C_2), 75.28–72.02 (C_3-C_5), 66.07 (C_{6s}), 63.48 (PDMAEMA), 59.76 (C_6), 55.84 (PDMAEMA), 44.85 (PDMAEMA), 44.48 (PDMAEMA), 19.84 (PDMAEMA), 19.36–18.03 (PDMAEMA), 16.41 (PDMAEMA). FT-IR (ATR) in cm^{-1}: $\tilde{\nu}$ = 1722 (C=O), 1205 around (S=O), 778 (S–O). Degree of substitution ascribed to sulfate group is DS_S = 0.54, while $DS_{PDMAEMA}$ is 0.28. Details of calculation methods of the DSs and $DS_{PDMAEMA}$ and elemental analysis results can be found in Supporting Information.

Preparation of poly(2(dimethylamino)ethyl methacrylate) (PDMAEMA)-grafted chitosan sulfate (P-CHS)

Chitosan sulfate acrylate (82.84 mg, 0.287 mmol, the details for the preparation of chitosan sulfate acrylate are included in Supporting Information) solution was added to PDMAEMA-SH in THF solution (0.25 g, 0.043 mmol). The synthetic procedure of P-CHS is the same as P-CS synthesis. ^{1}H NMR (400 MHz, D_2O) δ 4.56–4.43 (m), 4.31 (d), 4.12 (d), 3.90–3.47 (m), 2.89 (s), 2.67 (s), 2.28 (s),

1.95 (d), 1.11–0.84 (m). ^{13}C NMR (126 MHz, D_2O) δ 178.71 (PDMAEMA), 178.41 (PDMAEMA), 102.67 (C_1), 79.06–71.90 (C_2-C_5), 66.53 (C_{6s}), 63.48 (PDMAEMA), 60.21 ($_{C6}$), 56.01 (PDMAEMA), 19.54–15.70 (PDMAEMA). FT-IR (ATR) in cm^{-1}: $\tilde{\nu}$ = 3404 (O–H), 1718 (C=O), 1205 around (S=O), 1142 (C–N), 774 (S–O). Degree of substitution ascribed to sulfate group is $DS_S = 0.58$, while $DS_{PDMAEMA}$ is 0.31. Details of calculation methods of the DSs and $DS_{PDMAEMA}$ and elemental analysis results can be found in Supporting Information.

Preparation of hydrogels

Here we used polyacrylamide hydrogel as a substrate with high transparency and comparable mechanical properties. Meanwhile, P-CS or P-CHS was added inside of the hydrogel network and served as the stimulus-responsive unit. Typically, the hydrogels were constructed as follows.

P-CS hydrogel: A mixture of monomer acrylamide (0.14 g, 2 mmol), cross-linker *N, N′*-methylenebisacrylamide (MBA, 1.4 mg, 0.009 mmol), catalyst *N, N, N′, N′*-tetramethylethylenediamine (TEMED, 10 µL) and P-CS (20 mg) were mixed in 1 mL DI-water (pH 6.2–6.4, three times testing) and cooled in refrigerator (0 °C) for 30 min in advance. After that, ammonium persulfate (APS, 1 M, 8 µL) as initiator was added and the mixture was transferred to the mold quickly. The hydrogels were prepared promptly for 10 min and were stored under a saturated vapor environment for subsequent measurements.

P-CHS hydrogel: A mixture of monomer acrylamide (0.14 g, 2 mmol), cross-linker MBA (1.4 mg, 0.009 mmol), catalyst TEMED (10 µL) and P-CHS (20 mg) were mixed in 1 mL DI-water (pH 6.2–6.4, three times testing) and cooled in refrigerator (0 °C) for 30 min in advance. After that, APS (1 M, 8 µL) as initiator was added and the mixture was transferred to the mold quickly. The hydrogels were prepared promptly for 10 min and were stored under a saturated vapor environment for subsequent measurements.

The pure polyacrylamide hydrogel was set as the control hydrogel. The precursor solution compositions were the same as in the P-CS or P-CHS hydrogels, except for the absence of stimuli-responsive units.

Characterization

Elemental analysis

The elemental analysis was performed with an Elemental Analyzer Vario EL III CHN from Elementar (Hanau, Germany).

Ultraviolet–visible spectroscopy (UV–vis)

UV–vis measurements were carried out on Cary 300 UV–Vis Spectrophotometer (Agilent Technologies Deutschland GmbH, Germany). The transmittance at the wavelength of 600 nm was used to characterize the transparency of the films.

Nuclear magnetic resonance spectroscopy (NMR)

^{1}H NMR and ^{13}C NMR spectra were obtained on a Bruker Avance III 500 MHz spectrometer in deuterated solvents at 25 °C. 150 scans for ^{1}H NMR spectra and scans of up to 15,000 were accumulated for the ^{13}C NMR spectra. Chemical shifts are reported relative to the solvent peak.

Fourier transform infrared spectroscopy (FT-IR)

FT-IR spectra were recorded on Alpha FT-IR Spectrometer (Bruker, Germany) at room temperature. All samples were measured between 4000 and 500 cm^{-1} with a resolution of 4 cm^{-1} using Platinum ATR and accumulated 24 scans.

Gel permeation chromatography-size exclusion chromatography (GPC-SEC)

The molecular weight distribution of synthesized PDMAEMA oligomer was determined with a GPC-SEC Analysis Systems 1260 Infinity. THF was used as eluent with toluene (> 99.7%, dry, from Sigma-Aldrich) as internal standard (flow velocity 1.0 mL•min^{-1}). The system was calibrated with polystyrene standards.

Dynamic light scattering spectroscopy (DLS)

DLS measurements were performed on a Zetasizer Nano ZS (Malvern Instruments Ltd., UK) using 5

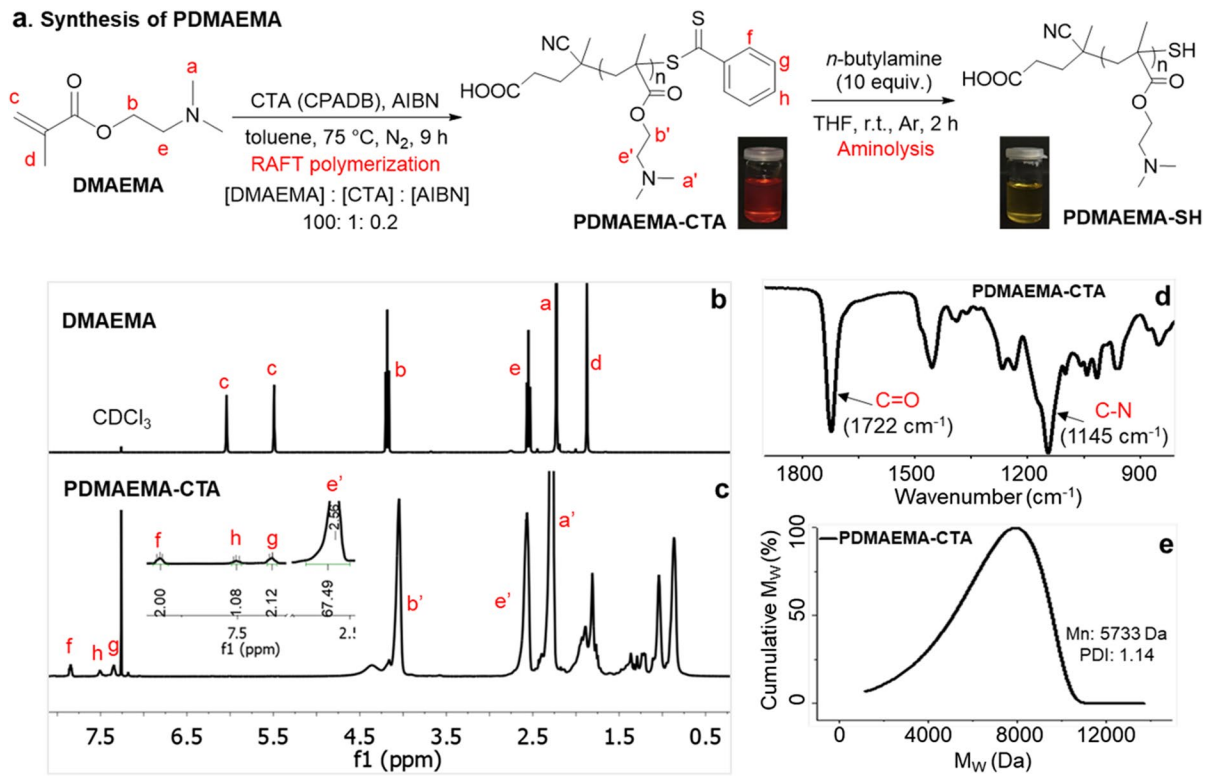

Fig. 1 **a** RAFT polymerization for the synthesis of PDMAEMA. ^{1}H NMR analysis of **b** DMAEMA and **c** PDMAEMA-CTA in $CDCl_3$ at room temperature. **d** FT-IR analysis of PDMAEMA-CTA. **e** Gel permeation chromatography analysis of PDMAEMA-CTA

Table 1 GPC analysis and NMR analysis of PDMAEMA-CTA

Name	Yield (wt%)	GPC analysis				^{1}H NMR analysis	
		M_n	M_w	PDI	Polymerization degree (n)[a]	M_w	Polymerization degree (n)[b]
PDMAEMA-CTA	29%	5733	6560	1.14	35	5146	31

[a]The degree of polymerization is calculated with the Mn by GPC analysis. [b]The degree of polymerization is calculated by ^{1}H NMR analysis

mW laser with the incident beam of 633 nm (He–Ne laser).

Scanning electron microscopy spectroscopy (SEM)

SEM measurements were performed on Leo SUPRA 35 (Carl Zeiss SMT GmbH, Oberkochen, Germany). Before the measurement, the hydrogels which were at RT or under equilibrium in water of 42 °C were promptly frozen in liquid nitrogen. Then, the gels were lyophilized to completely dehydrate without disturbing the internal porous structure of the hydrogels. Prior to SEM detection, the samples were properly cut and sputter-coated with gold-platinum (80/20).

Water contact angle

A DSA25 Drop Shape Analyzer (KRÜSS, Germany) was applied to measure the water contact angle of hydrogels. The water on the surface of hydrogel was removed using filter paper. Then the method of sessile drop was used. The volume of drop was set as 4 µL under the rate of 2.67 µL/s. The images were recorded

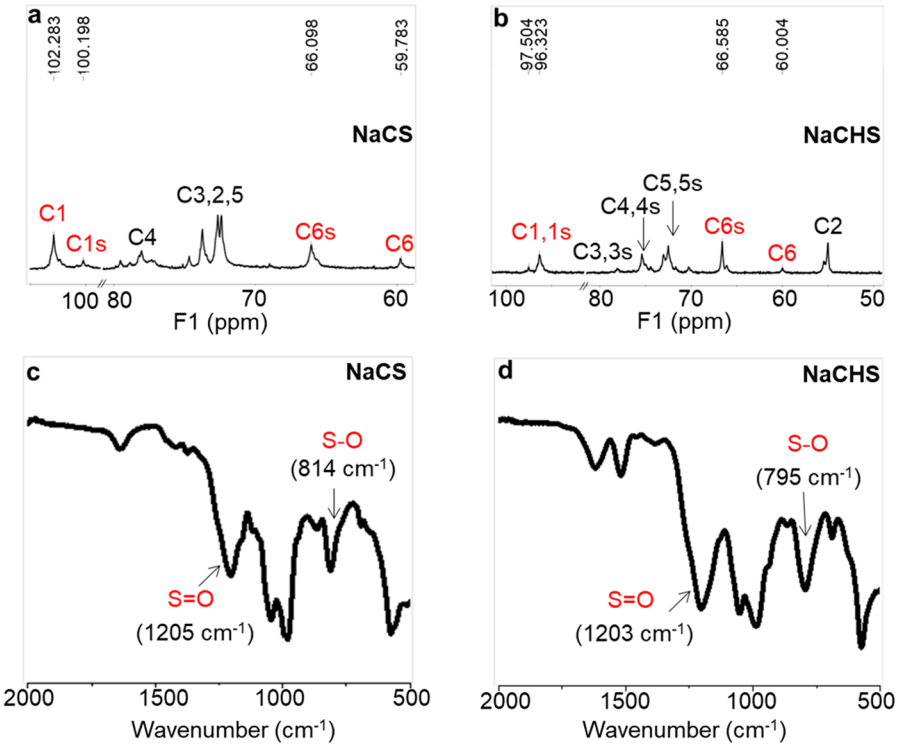

Fig. 2 ^{13}C NMR analysis of **a** NaCS and **b** NaCHS in D_2O at room temperature. FT-IR analysis of **c** NaCS and **d** NaCHS

and analyzed with the help of KRÜSS ADVANCE software.

The mechanical performance of hydrogels

The mechanical properties of hydrogels were determined using a Z3 micro tensile test machine (Grip-Engineering Thümler GmbH, Germany), equipped with a 50 N sensor. The crosshead speed was 6 mm/min and the deforming speed was 2.5% s^{-1}. The elastic modulus (E) was calculated as the slope of the nominal compression stress–strain curves within the strains range from 0 to 100%. The fracture energy of these gels is defined as

$$W = \frac{\int_0^{\varepsilon_k} F d\varepsilon}{A} \int_0^{\varepsilon_k} \sigma d\varepsilon$$

i.e., the area under the stress–strain curve.

Results and discussion

To prepare the hydrogels, the polymeric segments were synthesized at first. Chain transfer agent-containing PDMAEMA (PDMAEMA-CTA) was synthesized through reversible addition–fragmentation chain transfer (RAFT) polymerization. Resulting PEMAEMA-CTA (M_n: 5733 Da and M_w: 6560 Da, polydispersity index (PDI = M_w/M_n): 1.14) was further verified by gel permeation chromatography (GPC), nuclear magnetic resonance spectroscopy (NMR) and Fourier-transform infrared spectroscopy (FT-IR) analysis (Fig. 1 and Table 1) (Yao et al. 2016). The yellow PDMAEMA-SH was obtained through the following aminolysis of red PDMAEMA-CTA in THF solution (Fig. 1a, Fig. S8) (Yao et al. 2016).

In parallel, cellulose sulfate (CS) and chitosan sulfate (CHS) were prepared via the sulfation of cellulose and chitosan following previous methods (Zhang et al. 2010a, b). The structures of CS and CHS were characterized with elemental analysis, ^{13}C NMR and FT-IR analysis (Fig. 2 and Fig. S1-S2; Table S1-S2). Obtained CS and CHS were further modified into cellulose sulfate acrylate (CSA) and chitosan sulfate acrylate (CHSA), which were verified with $^{1}H/^{13}C$ NMR, elemental analysis, and FT-IR analysis (Fig. 3 and Fig. S3-S7; Table S3-S4). Finally, the final PDMAEMA-cellulose sulfate (P-CS) and

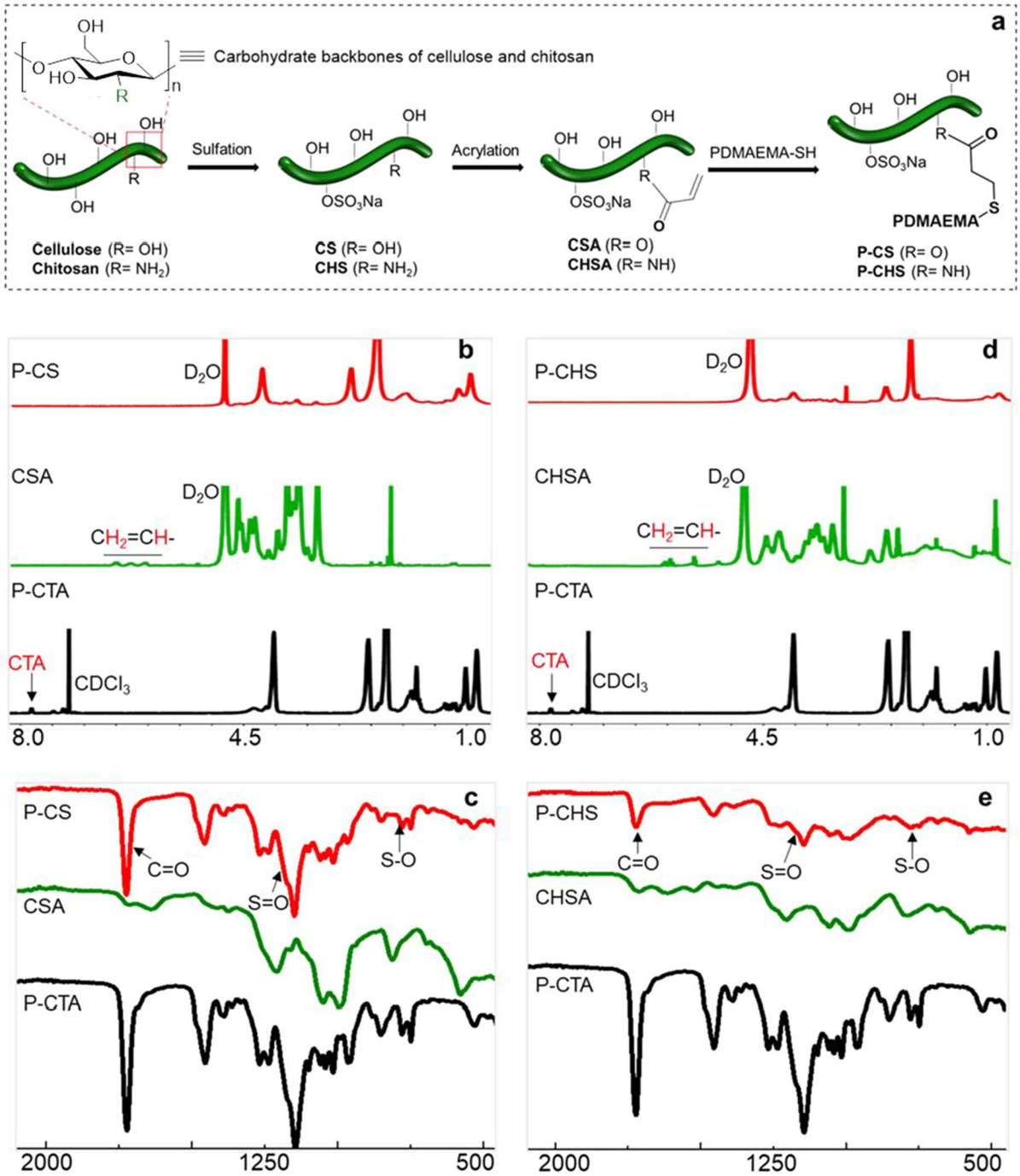

Fig. 3 **a** Schematic representation for the synthetic routes of P-CS and P-CHS. The degree of deacetylation (DD) of chitosan is 97.96% (DD: 97.96%). **b** ^{1}H NMR spectrum of the PDMAEMA-CS, CSA (cellulose sulfate acrylate) and PDMAEMA-CTA; **c** FT-IR spectrum of the PDMAEMA-CS, CSA (cellulose sulfate acrylate) and PDMAEMA-CTA; **d** ^{1}H NMR spectrum of the PDMAEMA-CHS, CHSA (chitosan sulfate acrylate) and PDMAEMA-CTA in D_2O at room temperature; **e** FT-IR spectrum of the PDMAEMA-CHS, CHSA (chitosan sulfate acrylate) and PDMAEMA-CTA

Table 2 The DS_S and $DS_{PDMAEMA}$ of P-CS and P-CHS

Starting materials	Samples	DS_S	$DS_{PDMAEMA}$
Cellulose	P-CS	0.54	0.28
Chitosan	P-CHS	0.58	0.31

The degree of sulfation/PDMAEMA grafting is presented as per repeat unit of sugar

PDMAEMA-chitosan sulfate (P-CHS) were prepared via a click reaction between PDMAEMA-SH and CSA/CHSA (Fig. 3).

The preparation of P-CS and P-CHS was confirmed by elemental analysis, NMR and FT-IR spectroscopy (Fig. 3 and Fig. S8-S14; Table S5-S6). First, the ^{1}H NMR signal of acrylate group in CSA disappeared after the click reaction (Fig. 3b), while the signals in aliphatic area of CSA and P-CTA could be found in the ^{1}H NMR spectrum of P-CS. Moreover, the characteristic signals ascribed to C=O, S=O and S–O bonds are visible within the FT-IR spectrum of P-CS (Fig. 3c). The P-CHS was also verified by ^{1}H NMR (Fig. 3d) and FT-IR spectroscopy (Fig. 3e). As well, similar characteristic signals of CHSA and P-CTA are visible in the ^{1}H NMR and FT-IR spectra of P-CHS. Based on the result of elemental analysis and ^{13}C NMR spectra (Table 2), the degrees of substitution of P-CS ascribed to sulfate group (DS_S) and PDMAEMA group ($DS_{PDMAEMA}$) are determined to be 0.54 and 0.28, respectively. Using the same calculation method, P-CHS with DS_S (0.57) and $DS_{PDMAEMA}$ (0.31) was obtained (Table 2).

Before the preparation of hydrogels, the thermoresponsive properties of P-CS and P-CHS solution were studied with dynamic light scattering (Fig. S15). The lower critical solution temperature (LCST) of P-CS and P-CHS can be determined in the particle size curves as shown in Fig. S15 (Lu et al. 2022). A slightly lower cloud point of P-CS can be found at 39 °C in comparison to the cloud point of P-CHS at 40 °C (Fig. S16). With increasing temperature up to 45 °C, the hydrodynamic radius (R^h) of P-CS obviously increased, while R^h of P-CHS slightly increased (Fig. S15).

After preparing these polysaccharide derivatives, ionic P-CS hydrogels were prepared for the first time by the polymerization of an aqueous solution containing P-CS, monomer acrylamide, initiator APS, catalyst TEMED and crosslinker MBA. Similar procedures were also used to prepare P-CHS hydrogels. P-CS and P-CHS hydrogels showed readily reversible thermoresponsive behaviors (Fig. 4). By increasing the temperature from 25 to 42 °C, the hydrogels turned opaque (Fig. 4c, h), while lowering the temperature reversibly resulted in transparent hydrogels (Fig. 4a, f). According to scanning electron microscope analysis (SEM), freeze-dried P-CS hydrogels contain a uniform porous structure (~2.5 um) at 25 °C (Fig. 4b). As expected, plunge freezing of hydrogels in liquid nitrogen could result in the formation of small ice crystals, which could induce the formation of small pores during the rapid cooling of the samples.(Paterson et al. 2013) In comparison, freeze-dried P-CS hydrogels at 42 °C showed only aggregated structure after freeze-drying (Fig. 4d). Compared to P-CS hydrogels, freeze-dried P-CHS hydrogels at 25 °C contained much smaller pores (~1 um) (Fig. 4g). When the temperature of P-CHS hydrogels was elevated from 25 to 42 °C, the pores became larger (~4 um) and they did not show significant collapsed aggregation (Fig. 4i).

The optical properties of P-CS hydrogels and P-CHS hydrogels were also demonstrated via UV–vis analysis based on their transmission of visible light at 25 °C and 42 °C (Fig. 4e and j). Firstly, the control hydrogels showed no thermally responsive properties (Fig. S17). P-CS hydrogels showed good transmittance of visible light at 25 °C. In comparison, the visible light transmittance of the P-CS hydrogels at 42 °C decreases only slightly, for example, 3% decrease from 25 to 42 °C at 600 nm (Fig. 4e). Compared to P-CS hydrogels, P-CHS hydrogels significantly blocked the transmission of visible light at 42 °C, for example, 34% decrease from 25 to 42 °C at 600 nm (Fig. 4j). Notably, P-CHS hydrogels displayed better performance than P-CS hydrogels in blocking light transmission at 42 °C based on their lower transmission of visible light. This could be caused by the more inhomogeneous distribution of aggregates in P-CHS compared to P-CS at 42 °C. It was further demonstrated with DLS analysis of the polymer in solution (Fig. S15). For example, although the hydrodynamic radius of P-CS was 10 times greater than that of P-CHS, the PDI of P-CS was half that of P-CHS (The PDI means the size distribution,

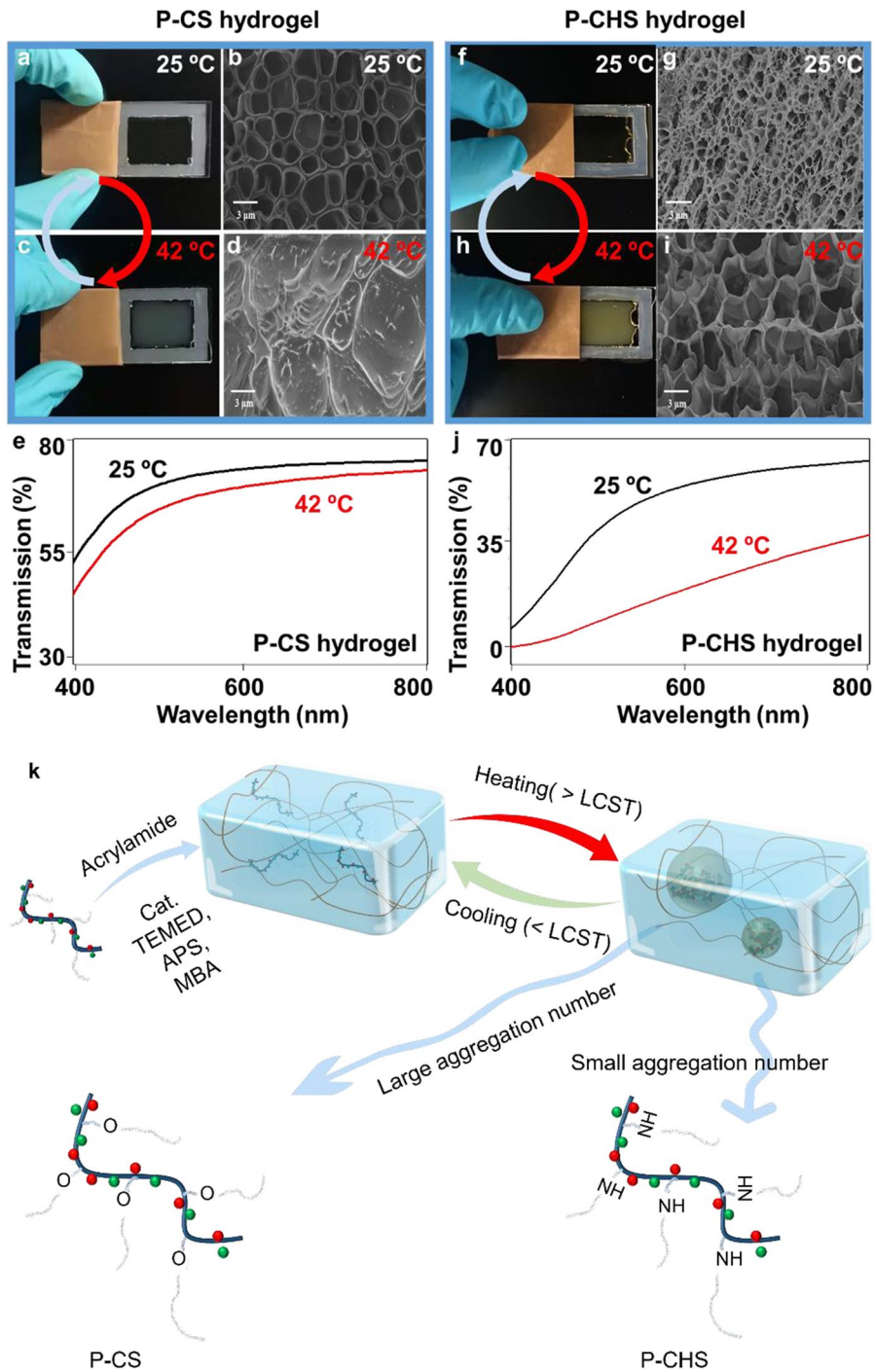

Fig. 4 Thermal properties of P-CS and P-CHS hydrogels. SEM and optical observation analysis of **a**–**d** P-CS hydrogels and **f**–**i** P-CHS hydrogels at 25 and 42 °C. Optical properties of **e** P-CS hydrogels and **j** P-CHS hydrogels at 25 °C (black line) and 42 °C (red line). **k** Different aggregation behaviors of P-CS and P-CHS hydrogels

obtained by DLS analysis). The observed optical properties of P-CS hydrogels and P-CHS hydrogels are in agreement with the thermoresponsive properties of P-CS and P-CHS hydrogels (Fig. 4a, c, f, and h).

These transparent hydrogels are not only thermoresponsive due to existing PDMAEMA grafted on CS/CHS, ionic polysaccharides also can be readily crosslinked, making the hydrogel network sensitive to temperature (Fig. 4 k) (Alvarez-Lorenzo et al.

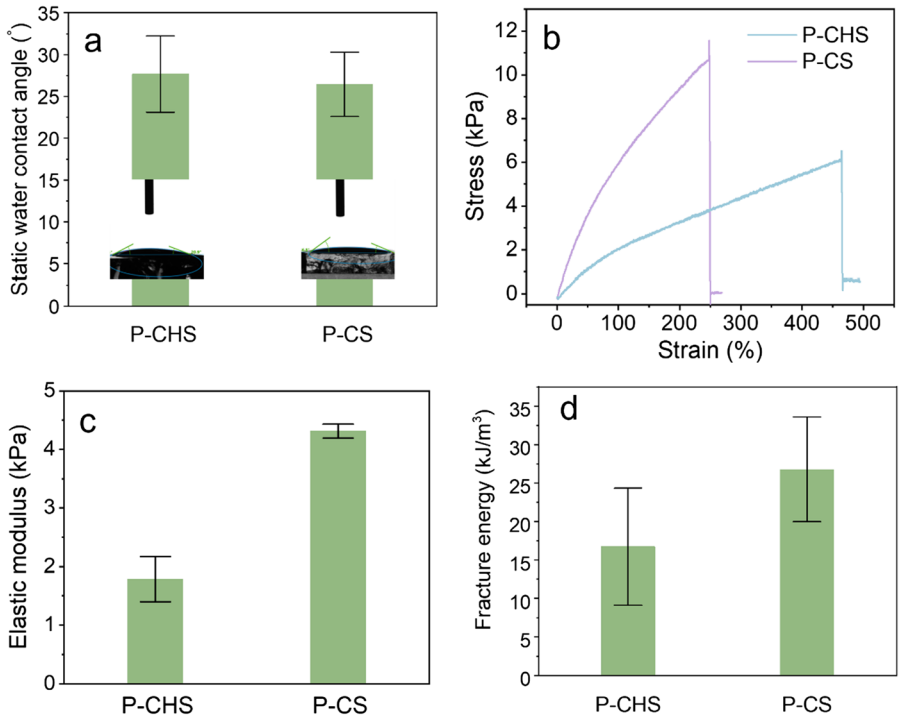

Fig. 5 **a** Static water contact angle of P-CHS and P-CS hydrogels; **b** Typical strain-stress curves of P-CHS and P-CS hydrogels at 25 °C; **c** The elastic modulus of P-CHS and P-CS hydrogels; **d** The facture energy of P-CHS and P-CS hydrogels. (n >3)

2013). Below LCST, the hydrogels have a transparent appearance based on the good solubility of ionic P-CS/P-CHS, as the intermolecular hydrogen bonding between the hydrophilic chains of PDMAEMA and water. The ion–dipole force among sulfate groups of P-CS/P-CHS and water molecules also contributes to the good solubility. After increasing the solution temperature above LCST, a cloud point appeared due to the disruption of polymer chains and water molecules, leading to the gradual chain folding and heat-induced aggregation (Van de Wetering et al. 1998). LCST behavior is generally driven by the varying hydrophobic domain of polymers depending on the temperature. Furthermore, the hydrophilic groups of polymers can affect the formation of aggregates and their sizes (Zeng et al. 2022). Specifically, the divergence between P-CS and P-CHS hydrogels was demonstrated to be mainly ascribed to the carbohydrate backbone difference between -O- and -NH-. Based on the DLS results (Fig. S15-S16) and optical observation analysis results (Fig. 4a, c, f, and h), -NH- could maintain a relatively better hydrophilicity compared to -O-, resulting in the smaller aggregation size of polymer chains and showing the inhomogeneous aggregation in P-CHS hydrogel at higher temperature. In contrast, -O- induced a large aggregation size of polymer chains with lower PDI in P-CS hydrogel when the temperature increased (The PDI means the size distribution, obtained by DLS analysis).

To evaluate interaction between water and various hydrogels, the static water contact angle (SWCA) of P-CHS and P-CS hydrogels were characterized. As shown in Fig. 5a, both P-CHS and P-CS hydrogels behaved similar SWCA of around 27°. These results indicated that P-CHS or P-CS hydrogels are hydrophilic, and the introduction of P-CHS or P-CS polymers only slightly affects the hydrophilicity of these hydrogels. To evaluate the effect of different carbohydrate backbones in P-CS and P-CHS hydrogels on mechanical performance, the mechanical properties of the hydrogels were recorded at 25 °C.

Figure 5b shows the representative tensile stress–strain curves of P-CHS and P-CS hydrogels. The P-CHS hydrogels showed an elongation at break (λ_k) up to 460%, while the λ_k of the P-CS hydrogels was less than 250%. This difference could be induced by different interactions between polymer matrix polyacrylamide and P-CHS/P-CS, which

were distinguished by amide and ester bonds, respectively. Compared with P-CHS hydrogels with an average elastic modulus of 1.79 ± 0.38 kPa, P-CS hydrogels demonstrated higher elastic modulus of 4.31 ± 0.12 kPa (Fig. 5c). These results suggested that the P-CS hydrogels were stronger and harder, compared to weaker and softer but more elastic P-CHS hydrogels. The fracture toughness of these gels is defined as the area under the stress–strain curve (Fig. 5d). It is interesting to find that the fracture energy of P-CS hydrogels was about 28.78 kJ/m^3, which was much higher than that of P-CHS hydrogels (16.74 ± 7.62 kJ/m^3). These results showed that P-CS hydrogels possessed better crack resistance capacity than P-CHS hydrogels. Furthermore, the higher elastic modulus and fracture energy of P-CS hydrogels indicate that the pore structure within P-CS hydrogels is more stable than that of P-CHS hydrogels at 25 °C.

Conclusion

In summary, PDMAEMA-grafted cellulose sulfate (P-CS) and PDMAEMA-grafted chitosan sulfate (P-CHS) were successfully synthesized through multi-step reactions. The P-CS and P-CHS polymers were further applied in crosslinked polyacrylamide networks, resulting in the P-CS and P-CHS hydrogels, respectively. In terms of morphology and optical analysis, both P-CS and P-CHS hydrogels were thermoresponsive and turned from transparent at 25 °C to opaque states at 42 °C. The P-CHS hydrogels showed an elongation at break (λ_k) up to 460%, while the elongation at break λ_k of P-CS hydrogel was less than 250%. Compared with the P-CS hydrogels, the P-CHS hydrogels blocked more strongly the transmission of visible light. Compared with P-CHS hydrogels, P-CS hydrogels showed higher elastic modulus and were stronger. The aforementioned properties of P-CS and P-CHS hydrogels provide strong support for different functions of their different carbohydrate backbones.

Acknowledgments We thank Sandra Lotze from P. Vana's group for her support by analysis.

Authors contributions KZ conceived the concept and supervised the project. KZ and DX performed the experiment, prepared the samples and did the analysis. YL and TG supported the analysis. PV provided the GPC measurements. KZeng drafted the manuscript. All authors discussed the results and revised the manuscript. KZ and DX contributed equally to this work.

Funding Open Access funding enabled and organized by Projekt DEAL. This work was carried out with support from the German Research Foundation (DFG) under Grant agreements ZH 546/3–1 and Gr 1290/12–1. K. Zeng and D. Xu thank China Scholarship Council for their PhD grants.

Declarations

Conflict of interest The authors declare no conflict of interest.

Ethics approval All authors have understood and complied with the code of ethics, approved, and agreed to participate.

Consent for publication All authors agreed to publish the paper.

References

Ahmed S, Ikram S (2017) Chitosan: derivatives, composites and applications: John Wiley & Sons.

Alvarez-Lorenzo C, Blanco-Fernandez B, Puga AM, Concheiro A (2013) Crosslinked ionic polysaccharides for stimuli-sensitive drug delivery. Adv Drug Deliv Rev 65:1148–1171. https://doi.org/10.1016/j.addr.2013.04.016

Bi S, Feng C, Wang M, Kong M, Liu Y, Cheng X, Chen X (2020) Temperature responsive self-assembled hydroxybutyl chitosan nanohydrogel based on homogeneous reaction for smart window. Carbohydr Polym 229:115557. https://doi.org/10.1016/j.carbpol.2019.115557

Coviello T, Matricardi P, Marianecci C, Alhaique F (2007) Polysaccharide hydrogels for modified release formulations. J Control Release 119:5–24. https://doi.org/10.1016/j.jconrel.2007.01.004

Ding Y, Yan Y, Peng Q, Wang B, Xing Y, Hua Z, Wang Z (2020) Multiple stimuli-responsive cellulose hydrogels with tunable LCST and UCST as smart windows. ACS Appl Polym Mater 2:3259–3266. https://doi.org/10.1021/acsapm.0c00414

Doberenz F, Zeng K, Willems C, Zhang K, Groth T (2020) Thermoresponsive polymers and their biomedical application in tissue engineering–a review. J Mater Chem B 8:607–628. https://doi.org/10.1039/C9TB02052G

Dragan ES, Dinu MV (2019) Polysaccharides constructed hydrogels as vehicles for proteins and peptides. A review. Carbohydr Polym 225:115210. https://doi.org/10.1016/j.carbpol.2019.115210

Hettrich K, Wagenknecht W, Volkert B, Fischer S (2008) New possibilities of the acetosulfation of cellulose. Macromol Symp 262:162–169. https://doi.org/10.1002/masy.200850216

Hoffman AS (2013) Stimuli-responsive polymers: biomedical applications and challenges for clinical translation. Adv Drug Deliv Rev 65:10–16. https://doi.org/10.1016/j.addr.2012.11.004

Kabir S, Sikdar PP, Haque B, Bhuiyan M, Ali A, Islam M (2018) Cellulose-based hydrogel materials: chemistry, properties and their prospective applications. Prog Biomater 7:153–174. https://doi.org/10.1007/s40204-018-0095-0

Ke Y, Chen J, Lin G, Wang S, Zhou Y, Yin J, Long Y (2019) Smart windows: electro-, thermo-, mechano-, photochromics, and beyond. Adv Energy Mater 9:1902066. https://doi.org/10.1002/aenm.201902066

Klouda L, Mikos AG (2008) Thermoresponsive hydrogels in biomedical applications. Eur J Pharm Biopharm 68:34–45. https://doi.org/10.1016/j.ejpb.2007.02.025

Li H-J, Jiang H, Haraguchi K (2018) Ultrastiff, thermoresponsive nanocomposite hydrogels composed of ternary polymer–clay–silica networks. Macromolecules 51:529–539. https://doi.org/10.1021/acs.macromol.7b02305

Lu Y-T, Zeng K, Fuhrmann B, Woelk C, Zhang K, Groth T (2022) Engineering of stable cross-linked multilayers based on thermo-responsive PNIPAM-grafted-chitosan/heparin to Tailor their physiochemical properties and Biocompatibility. ACS Appl Mater Interfaces 14:29550–29562. https://doi.org/10.1021/acsami.2c05297

Lu Y-T, Hung P-T, Zeng K, Woelk C, Fuhrmann B, Zhang K, Groth T (2023) Surface properties and bioactivity of PNIPAM-grafted-chitosan/chondroitin multilayers. Smart Mater Med 4:356–367. https://doi.org/10.1016/j.smaim.2022.11.008

Ma GH, Nagai M, Omi S (2001) Study on preparation of monodispersed poly (styrene-co-N-dimethylaminoethyl methacrylate) composite microspheres by SPG (Shirasu Porous Glass) emulsification technique. J Appl Polym Sci 79:2408–2424. https://doi.org/10.1002/1097-4628(20010328)79:13%3c2408::AID-APP1048%3e3.0.CO;2-Q

Meeussen F, Nies E, Berghmans H, Verbrugghe S, Goethals E, Du Prez F (2000) Phase behaviour of poly (N-vinyl caprolactam) in water. Polymer 41:8597–8602. https://doi.org/10.1016/S0032-3861(00)00255-X

Okano T, Yamada N, Sakai H, Sakurai Y (1993) A novel recovery system for cultured cells using plasma-treated polystyrene dishes grafted with poly (N-isopropylacrylamide). J Biomed Mater Res 27:1243–1251. https://doi.org/10.1002/jbm.820271005

Paterson SM, Casadio YS, Brown DH, Shaw JA, Chirila TV, Baker MV (2013) Laser scanning confocal microscopy versus scanning electron microscopy for characterization of polymer morphology: sample preparation drastically distorts morphologies of poly (2-hydroxyethyl methacrylate)-based hydrogels. J Appl Polym Sci 127:4296–4304. https://doi.org/10.1002/app.38034

Rawlinson L-AB, Ryan SM, Mantovani G, Syrett JA, Haddleton DM, Brayden DJ (2010) Antibacterial effects of poly (2-(dimethylamino ethyl) methacrylate) against selected gram-positive and gram-negative bacteria. Biomacromol 11:443–453. https://doi.org/10.1021/bm901166y

Schmolka IR (1972) Artificial skin I. Preparation and properties of pluronic F-127 gels for treatment of burns. J Biomed Mater Res 6:571–582. https://doi.org/10.1002/jbm.820060609

Stamm AJ (1964) Wood and cellulose science. Wood Cellul Sci

Van de Wetering P, Zuidam N, Van Steenbergen M, Van Der Houwen O, Underberg W, Hennink W (1998) A mechanistic study of the hydrolytic stability of poly (2-(dimethylamino) ethyl methacrylate). Macromolecules 31:8063–8068. https://doi.org/10.1021/ma980689g

Vrhovski B, Weiss AS (1998) Biochemistry of tropoelastin. Eur J Biochem 258:1–18. https://doi.org/10.1046/j.1432-1327.1998.2580001.x

Wang J, Song D, Jia S, Shao Z (2014) Poly (N, N-dimethylaminoethyl methacrylate)/graphene oxide hybrid hydrogels: pH and temperature sensitivities and Cr (VI) adsorption. React Funct Polym 81:8–13. https://doi.org/10.1016/j.reactfunctpolym.2014.03.013

Wang X, Yang Y, Huang H, Zhang K (2020) Temperature-responsive, manipulable cavitary hydrogel containers by macroscopic spatial surface-interior separation. ACS Appl Mater Interfaces 13:1573–1580. https://doi.org/10.1021/acsami.0c19448

Xiong M, Gu B, Zhang J-D, Xu J-J, Chen H-Y, Zhong H (2013) Glucose microfluidic biosensors based on reversible enzyme immobilization on photopatterned stimuli-responsive polymer. Biosens Bioelectron 50:229–234. https://doi.org/10.1016/j.bios.2013.06.030

Yang Y, Lu YT, Zeng K, Heinze T, Groth T, Zhang K (2021) Recent progress on cellulose-based ionic compounds for biomaterials. Adv Mater 33:2000717. https://doi.org/10.1002/adma.202000717

Yao H, Wei D, Che X, Cai L, Tao L, Liu L, Chen G-Q (2016) Comb-like temperature-responsive polyhydroxyalkanoate-graft-poly (2-dimethylamino-ethylmethacrylate) for controllable protein adsorption. Polym Chem 7:5957–5965. https://doi.org/10.1039/C6PY01235C

Zainal SH, Mohd NH, Suhaili N, Anuar FH, Lazim AM, Othaman R (2021) Preparation of cellulose-based hydrogel: a review. J Mater Res Technol 10:935–952. https://doi.org/10.1016/j.jmrt.2020.12.012

Zeng K, Groth T, Zhang K (2019) Recent advances in artificially sulfated polysaccharides for applications in cell growth and differentiation, drug delivery, and tissue engineering. ChemBioChem 20:737–746. https://doi.org/10.1002/cbic.201800569

Zeng K, Doberenz F, Lu Y-T, Nong JP, Fischer S, Groth T, Zhang K (2022) Synthesis of thermoresponsive PNIPAM-grafted cellulose sulfates for bioactive multilayers

via layer-by-layer technique. ACS Appl Mater Interfaces 14:48384–48396. https://doi.org/10.1021/acsami.2c12803

Zhang K, Brendler E, Fischer S (2010a) FT Raman investigation of sodium cellulose sulfate. Cellulose 17:427–435. https://doi.org/10.1007/s10570-009-9375-0

Zhang K, Helm J, Peschel D, Gruner M, Groth T, Fischer S (2010b) NMR and FT Raman characterisation of regioselectively sulfated chitosan regarding the distribution of sulfate groups and the degree of substitution. Polymer 51:4698–4705. https://doi.org/10.1016/j.polymer.2010.08.034

Zhang Z, Chen Z, Wang Y, Zhao Y (2020) Bioinspired conductive cellulose liquid-crystal hydrogels as multifunctional electrical skins. Proc Natl Acad Sci USA 117:18310–18316. https://doi.org/10.1073/pnas.200703211

Zhang K, Peschel D, Brendler E, Groth T, Fischer S (2009) Synthesis and bioactivity of cellulose derivatives. Macromol Symp 280:28–35. https://doi.org/10.1002/masy.200950604

Zou P, Yao J, Cui Y-N, Zhao T, Che J, Yang M, Gao C (2022) Advances in cellulose-based hydrogels for biomedical engineering: a review summary. Gels 8:364. https://doi.org/10.3390/gels8060364